Part V
Microstructured Reactors

14
Homogeneous Reactions

Volker Hessel and Patrick Löb

Homogeneous reactions as considered here comprise the class of liquid- and gas-phase reactions and exclude solid–liquid and solid–gas processes, i.e. heterogeneously catalyzed reactions with one homogeneous phase. The chapter covers the main engineering trends for homogeneous reactions, showing in which way and to what extent processes can be intensified by using microprocess technology and by which means this is done. First, the main engineering benefits which can be gained by using microprocess technology are listed, then the impacts of residence time distribution, mixing and heat transfer are discussed, and finally scale-out measures are introduced.

14.1
Benefits

14.1.1
Reaction Engineering Benefits

Homogeneous reactions as considered here are liquid- and gas phase reactions, and exclude multi-phase reactions and reactions with heterogeneous catalysts.

The majority of effects of microprocess technology are devoted to dimensional effects when shrinking down reaction volumes, in particular to their large surface-to-area ratio, small characteristic length and small internal volumes [1].

As initially proven by scouting experiments and increasingly understood by theoretical modeling, microreactor operation has benefits for reaction engineering due to well-defined and predictable laminar flows and enhanced mass and heat transfer at short overall processing times [2]. High selectivity saves on raw material consumption and facilitates separation issues. High conversion is a consequence of applying harsher conditions and/or the above-given features and, e.g., reduces recycling. The small internal volume facilitates the handling of hazardous materials and also cleaning or aseptic processing in the manufacture of biotech and pharmaceutical products. The small internal volume also permits fast parameter changes.

Micro Process Engineering, Vol.1: Fundamentals, Operations and Catalysts
Edited by V. Hessel, A. Renken, J.C. Schouten, and J.-I. Yoshida

ISBN: 978-3-527-31550-5

Novel process windows are opened, e.g. with regard to high-temperature and high-pressure processing or operation in the explosive regime (see Section 14.5).

In consequence, the above-mentioned intensified processing impacts many of the different parameters specifying processing and products, e.g. the number average of the molecular weight distribution or the polydispersity index in the case of polymerizations, and the particle size, shape and morphology in the case of functional materials such as polymer, pigment or inorganic particles [3]. For photochemical reactions, the quantum yield is a key property which is influenced by liquid layer miniaturization. Since the number and spread of parameters are very large, such information has to be looked up in specialized literature or starting from a review article in the field.

Other special reaction engineering benefits are gained in the field of energy generation, e.g. concerning fuel microprocessors or microcombustors [4, 5]. Benefits of energy efficiency, low pressure drop due to the laminar flow regime, system integration, e.g. by integrated heat exchanger reactor design, compactness and improvement of system dynamics, e.g. by fast start-up, have been reported. Similar specific parameters will be introduced in the food, personal care and consumer care industries, which are just at the beginning of taking up microstructured reactors.

14.1.2 Process Engineering Benefits

Process engineering benefits are not as well investigated and proven as their reaction engineering counterparts, as the latter deal with pilot processes and plants, usually performed at an industrial site, which are less frequent and rarely reported in detail. Process engineering occurs at a later stage of the value-added chain and is more complex in information and more difficult to quantify (not by using just one property) [4]. Hence it remains to future investigations to provide more information here.

Process engineering benefits are dedicated to improvements on a plant and process level [4]. Modularity of microprocess plants provides flexibility for different syntheses, which is a requirement especially for some fine chemical and pharmaceutical plants. Easy scalability, e.g. via the numbering-up concept, leads to short times to market, i.e. the chemically made products are introduced earlier to the end-user and development costs are reduced. Microprocess plants may have small CAPEX costs at reduced plant footprint, especially if there is a chance for large process intensification of the process under consideration. Legislation of chemical plants may take a considerable time in development and is part of the above-mentioned time-to-market period. Although not proven by a large number of examples, it stands to reason that microchemical plants bear the potential for fast authority approval, since processes may be highly simplified, authorization may start immediately after laboratory investigations (numbering-up: no change in processing to pilot and production) and safety measures are considerably reduced. Microchemical plants may have high shares of operation as compared with plant shutdown, because operation can be started and stopped rapidly (small internal volumes, fast response times, fast cooling). In the case of reversible (screwed or

clamped) interconnection, cleaning should be facilitated and also most microstructured reactors are of a plate-type design which, after dismantling, is open for any surface treatment. The latter does not necessarily hold for irreversible (e.g. laser-welded or brazed) interconnected microstructured reactors.

As a consequence out of all this, microprocess technology opens up routes to new supply chain management and business models and has the potential to change customer–deliverer relationships and the nature and functionality of products, e.g. by the concept of distributed production as opposed to central production ("world-scale plants") (see, e.g., [6, 7]). This may include providing an improved market position of process developing R&Ds as compared with contract manufacturers and large chemical companies. The process engineering benefits are not only related to chemistry as the current core market, but also can be implemented in other market sectors such as foods, personal care, consumer goods and energy technology.

14.2
Reactor Concepts – the Tools for Process Intensification

14.2.1
Micromixers, Micro Heat Exchangers and Minitubes/Capillaries

Two main motivations for using microprocess technology for homogeneous reactions are to speed up mixing and to transfer heat (most often to cool exothermic reactions). Thus, micromixers [8] and micro heat exchangers [9] are the constituent components [2, 4, 10]. The main advantage of separate mixing and cooling devices is that the characteristic mixing time (see the definition of Guichardon and Falk [11]) and the characteristic cooling time can be adapted to the corresponding characteristic reaction time. Simple definitions for a characteristic mixing time and cooling/heating time are given below.

$$t_m \propto L^2/D \tag{14.1}$$

where t_m is the characteristic mixing time, L the length for diffusion and D the diffusion constant. Assuming that $D = 10^{-9}\,m^2\,s^{-1}$ and $L = 10^{-5}\,m$ (10 μm), which is a typical lamella width, a mixing time of 100 ms results.

$$t_h \propto L^2/\chi;\ \chi = \lambda/(\rho c_p) \tag{14.2}$$

where t_h is the characteristic heating time, L the length for diffusion, χ the temperature diffusion coefficient, λ the heat conductivity, ρ the density and c_p the specific heat.

Concerning micro heat exchangers, it has been found, however, that due to the long period of operation needed for heat transfer and reaction (compared with mixing) and pressure loss considerations, minitubes/capillaries are often used to

replace micro heat exchangers, which have restrictions on maximum length. Since sometimes the effects of mixing and heat exchange are coupled or since the impact of mixing is simply unknown, micromixers are added upstream of micro heat exchangers or minitubes/capillaries, which are the most commonly found microprocess flow configurations for homogeneous reactions, especially when done in the liquid phase [10].

Gas-phase operation often uses premixed gases, which have to be heated to the reaction temperature. Owing to the faster reactions for gas-phase processes, typically being on the second scale, micro heat exchangers are proper reactor solutions [9].

14.2.2 Integrated Reactors

In a few cases with high demands on mixing and heat transfer, typically for very fast reactions which are of the order of the mixing time (<1 s), customized integrated micromixer–micro heat exchanger systems were developed [2, 4]. These systems are also demanded when dealing with explosive reactions where expansion of the inner volume between the process units is forbidden.

Some generic flow sheets comprising the reactor solutions in Sections 14.3.1 and 14.3.2 for liquid-phase homogeneous reactions are given in [8] (see Figure 14.1).

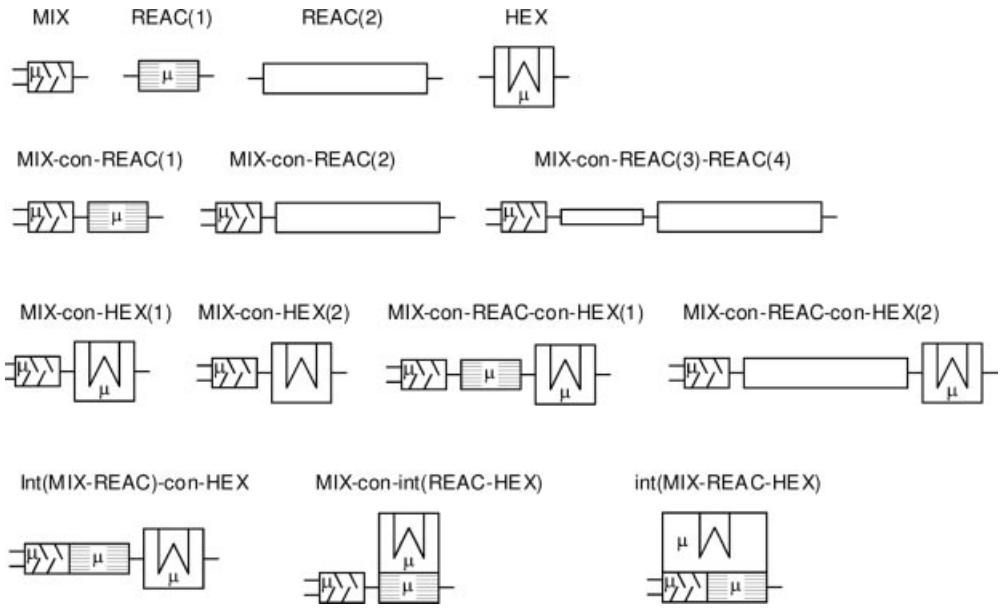

Figure 14.1 Generic reactor configurations for homogeneous liquid-phase reactions comprising micromixers (MIX), micro heat exchangers (HEX) and microreactors (REAC) in integrated (int) or connected (con) fashion. Reprinted with permission from *Chemistry Today* [10].

14.3
Reaction Optimization

14.3.1
Process Parameters with Impact on Reactor Performance

Reactor performance in terms of selectivity and conversion or space–time yield depends on the hydrodynamics, mass and heat transfer of the process (see, e.g., the literature cited in [2]). In the following, the impact of the residence time distribution, mixing and heat transfer is discussed, either from the viewpoint of modeling or where available illustrated with examples.

14.3.2
Residence Time Distribution

The influence of residence time distribution (RTD) on performance, selectivity and yield is the same in microreactors as in conventional reactors. Therefore, the effects are well understood. Nonetheless, the demonstration of this at the microscale has hardly been reported so far. However, some experimental techniques have been developed to measure RTDs in microchannel flows which allow comparison between different types of flows or flows run at different parameters so that at least optimal flow conditions with regard to RTD can be found.

Laminar flows in microchannels with their parabolic velocity profiles face superposition by radial and axial diffusion, as described by Taylor and Aris [61], introducing a global axial dispersion coefficient D_{ax} which is used as a parameter in their dispersion model [12]:

$$D_{ax} = D_m + \chi \frac{\mu^2 {d_t}^2}{D_m} \qquad (\chi = 1/192 \text{ for round tubes}) \tag{14.3}$$

where D_{ax} is the axial dispersion coefficient, D_m is the molecular diffusion coefficient, μ is the dynamic viscosity, and χ is a constant depending on the geometry of the channel (tube).

Following the dispersion model, RTD can be characterized by the Bodenstein number, *Bo*:

$$Bo = \frac{\bar{u}\, L}{D_{ax}} = Pe_{ax} \frac{L}{d_t} \tag{14.4}$$

where Pe_{ax} is the axial Peclet number, L is the length of the channel (tube) and d_t is the tube diameter.

For typical lengths of microchannels in the range of a few centimeters and average residence time in the range of a few seconds, axial back-diffusion is negligible, so that RTD is governed by the ratio of radial diffusion time to the fluid dynamic residence time [12]:

$$Bo \cong 192 \frac{D_m}{{d_t}^2} \frac{L}{\bar{u}} = 48 \frac{\tau}{t_{D,rad}} \tag{14.5}$$

where τ is the fluid dynamic residence time, L is the length of the channel (tube) and $t_{D,rad}$ is the radial diffusion time.

At constant fluid dynamic residence time, the RTD becomes narrower with decreasing channel dimension and thus decreasing diffusion time. The ratio of fluid dynamic residence time to radial diffusion time describes the Fourier number, *Fo*, which is a measure of the intensity of the radial molecular diffusion and thus radial mixing in den channels [12]:

$$Fo = \frac{\tau}{t_{D,rad}} = \frac{D_m}{R_t^2}\frac{L}{\bar{u}} \tag{14.6}$$

where R_t is the tube Radius.

For $Bo \geq 100$, the RTD approaches an ideal tube with plug flow which is given for laminar flows at $Fo > 2$.

An empirical relation for the half-width $\Delta t_{1/2}$ of the response signal of a pulse marking can be estimated from the Fourier number and fluid dynamic residence time [12]:

$$\Delta t_{\frac{1}{2}} \cong 0.024 \tau Fo^{-0.15} \tag{14.7}$$

14.3.2.1 RTD Studies on Liquid-phase Flows

One method for measuring RTDs in liquid flows uses a piezoelectrically actuated sample injector which releases 100 nL of tracer liquid into a microchannel of rectangular cross-section and compares single liquid with segmented gas–liquid flows [13]. The broadening of this tracer pulse is monitored by fluorescence microscopy measurements. A fluorescently labeled tracer pulse (reasonably representing the ideal Dirac δ function) is injected into a liquid stream through a transverse side-stream and then the flow is passed through a meandering channel. The average liquid segment lengths in the segmented flows were approximately $1 \times d_h$ and the average gas bubble length was approximately $4 \times d_h$ (where d_h is the channel hydraulic diameter).

For residence times up to several minutes (and same reaction time of the synthesis in microreactors), the insertion of large Taylor gas bubbles into a liquid flow reduces RTD broadening, since the liquid volumes are then segmented and have less axial dispersion (see Figure 14.2). The RTD of the segmented gas–liquid microflows is significantly narrower than for the single-phase liquid flow.

A simulation study was concerned with RTD broadening in the liquid phase in capillary residence tubes following a microreactor [14]. Such information was used for sequential organic synthesis in one capillary by means of appropriate setting of reactant flows and spacing fluid flows in order to avoid intermixing of the reactant flow pulses. The residence time distribution was calculated from a straightforward numerical model which neglects axial gradients. The results were verified experimentally using toluene as tracer. By applying the model to the sequential synthesis, the amount of sample fraction collected and the degree of dilution from the spacer liquid could be calculated, e.g. 77% collected volume at only 1.3% dilution in an optimized case. The reactant pulses were longer than 10 min.

In an experimental RTD study, pulse marking was performed with a dye tracer [15]. For this, a specially constructed microstructured injection unit was used. The tracer

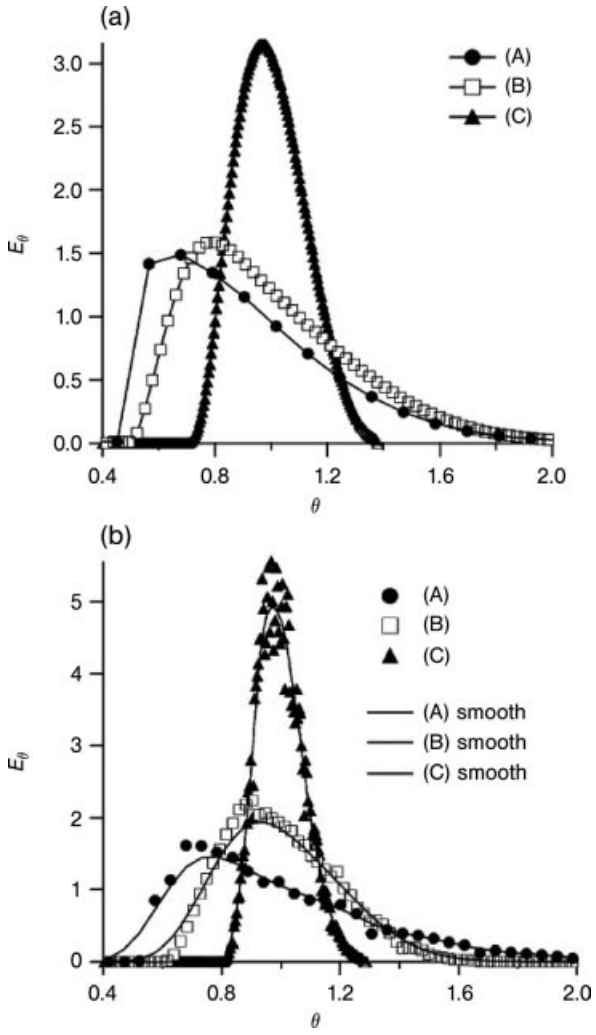

Figure 14.2 (a) RTD curves for single-phase flow, $j_L = 0.0096\ m\ s^{-1}$, (A) $L_1 = 20\ mm$ ($L/d_h = 112$), (B) $L_2 = 150\ mm$ (835) and (C) $L_3 = 1063\ mm$ (5948); (b) RTD curves for segmented flow condition B with $j_L = 0.0036\ m\ s^{-1}$, $j_G = 0.0252\ m\ s^{1}$, (A) $L_1 = 20.0\ mm$ ($99L/d_h$), (B) $L_2 = 149.2\ mm$ (738) and (C) $L_3 = 1062.6\ mm$ (5262). j_G and j_L are the superficial gas and liquid velocities, respectively, L is the channel length and i denotes the downstream position which is specified. Reprinted with permission from Elsevier [13].

concentration was detected by analyzing the transmittance with a laboratory-developed transmittance detection unit. The residence time distributions obtained were compared with common RTD models. The fit of an axial dispersion model to the experimental results was good when comparing the flow in the capillary only but was insufficient when adding a micromixer in front of the capillary. The same holds for a CSTR model. Several reasons were proposed to explain the deviation between the

model and experiment, e.g. dead volumes and non-ideal pulse introduction. This shows the need for a proper model developed for real-case multi-stage microreactor process designs.

Flow and residence time distributions were performed for a mesh microreactor, with the mesh separating and providing a contact area for two fluids [16]. An analytical resistance network method that is based on the analogy of viscous flow to networks of electrical resistances was applied to identify possible reactor plate geometries. The method was used to produce a reactor plate geometry that results in a uniform residence time distribution within the active mesh region while minimizing the non-active volume on the plate and the reactants' collecting channel. An acid–base reaction with color change served for visualizing the flow distribution in different plate geometries and agreed qualitatively with the theoretical results.

A non-intrusive method for RTD characterization has been claimed [17], which has been proven already for visualization of velocity fields in microchannels [18]. A photo-activated fluorescent dye dissolved in an aqueous solution is introduced continuously into a flow. A defined section of the inlet channel is exposed to a UV pulse to activate the tracer, which turns fluorescent. Due to this "inside" start of the pulse experiment, artifacts from peripheral equipment can be eliminated. The method generates almost ideal input signals, which simplifies the numerical treatment of experimental data. The new approach was found to be superior to various traditional injection methods. The ideal shape of the stimulus signal was demonstrated for an analytically well-defined straight channel and compared with a signal derived from deconvolution of non-ideal input signals [19].

14.3.2.2 **RTD Studies on Gas-phase Flows**

An RTD study on gas flows in a microchannel reactor specially designed for periodic operation with a γ-alumina catalyst deposited on the reactor channels was performed [20]. Argon (in nitrogen) was used as a tracer. The concentration of argon was determined by mass spectrometry every 30 ms.

Although the flow in the microchannels is laminar, a uniform radial concentration profile and consequently a narrow residence time distribution were obtained. Depending on the method used for manufacturing the microchannels, the Bodenstein number was found to be $Bo = ud/D_m \approx 70$ and consequently the microreactor behaves almost like a plug-flow reactor. The catalytic coating had no influence on this distribution, indicating a uniform deposition of the catalyst within the microchannels (see Figure 14.3).

Residence time distributions for a gas-phase flow through a microstructured falling film reactor were determined in order to develop an appropriate flow model for further study of gas-phase mass transfer characteristics in the system [21]. For the gas-phase residence time distribution experiments, the detection system involves a flow of oxygen-containing ozone as a tracer gas with continuous monitoring of the concentration by UV absorption. UV sensors exhibit very short response times, which are beneficial for high-frequency automated data acquisition in view of the short residence times in microreactors. Ozone can be simply generated *in situ* from oxygen by application of an electric field.

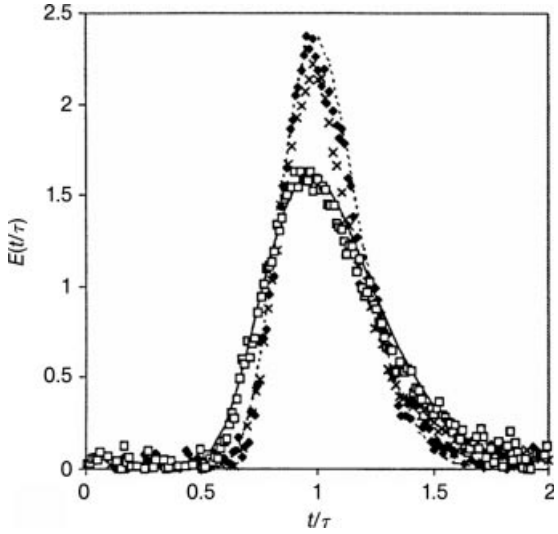

Figure 14.3 Residence time distribution in different microreactors: ◆, glued reactor without coating; ×, glued reactor with coating; □, reactor with graphite joints. Theoretical RTD curves for tubular reactors with (solid line) $Bo = 33$ and (dotted line) $Bo = 70$. Reprinted with permission from Elsevier [20].

The comparison of the experimental results with computational fluid dynamics calculations of the gas flow indicates a clear correlation of the flow model behavior with the appearance of recirculation loops in the reaction chamber and the effect of the gas jet at the entrance of the gas–liquid contact zone (Figure 14.4). The latter considerably increases the mixing in the gas phase and prevents the development of plug-flow behavior in the gas phase.

14.3.3 Impact of Mixing

If the reaction rate is so fast that it approaches the mixing rate, spatial concentration profiles within the microchannel exist which impact the course of reaction. Thus, for fast reactions, mixing efficiency is essential. Today's micromixers have mixing times typically in the range of some tens to hundreds of milliseconds; a few advanced mixers may even mix in a few milliseconds or less. It may happen even using this equipment that reactions are mixing sensitive. Further, one may exploit deliberately the ordered concentration profiles in laminar-flow microreactors for means of process optimization. The latter is in order to have control over diffusion by arranging solutes in predefined and regular fluid compartments and using kinetic relationships, i.e. the reaction order dependence of each reactant concentration. In the following, laminated or segmented fluid arrangements in microchannels of varying shape are considered. If a solid catalyst is further involved in the reaction, the reactants can be set initially far from or close to the catalyst for a bilayered flow, which impacts selectivity.

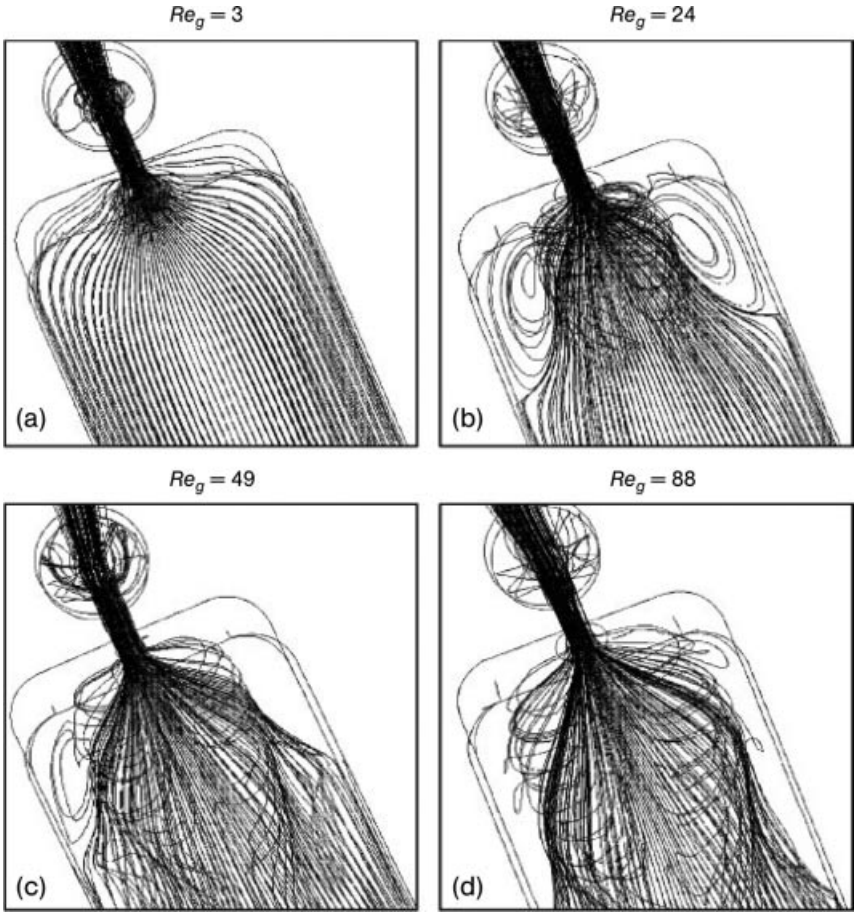

Figure 14.4 Flow path lines at the entrance of the gas–liquid contact zone of a falling film microreactor for Reynolds numbers of the gas flow of 3, 24, 49 and 88. Reprinted with permission from Elsevier [21].

The selectivity performance of bilayered reacting fluid arrangements was investigated by CFD simulations for four types of multiple reactions, differing in the type of side and follow-up reactions [22]. The effects of lamination width and rate constant on the yield of desired product as a function of conversion were determined. Lamination width has a pronounced effect on yield and selectivity, as is to be expected. In addition, the case of a perfect mixed (premixed) solution was considered, which gives higher yields compared with reactants fed as lamination segments. An exception occurs, however, when the rate constant for the desired product is much smaller than that converting the desired product by a follow-up reaction and when the order of the former reaction is less than that of the latter. In this case, the feed with the large lamination width shows a higher yield of the desired product than the perfectly mixed feed. Such results provide effective

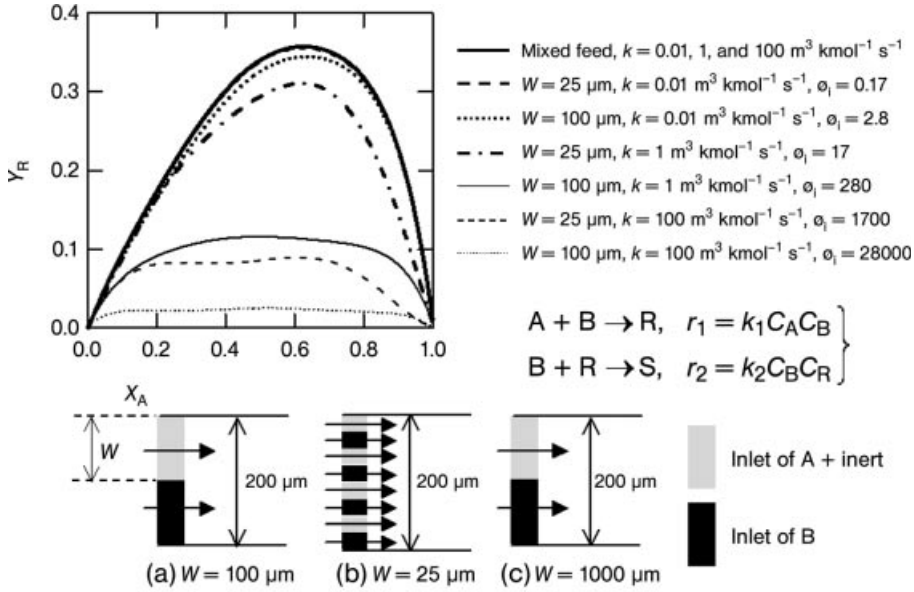

Figure 14.5 Relation between yield of R (Y_R) and conversion of A (X_A) for a consecutive reaction with different rate constants and lamination widths in different configurations of lamellae. Reprinted with permission from Elsevier [22].

information for the design of microreactors and of the measurement system of rate constants of multiple reactions.

In Figure 14.5, the yield dependence is plotted as a function of the rate constant and the lamination width for a pure consecutive-competing reaction scenario, A + B → R, B + R → S, with both rate constants assumed to be the same.

Reactant B is in two-fold excess over A to allow the reaction proceed as A + 2B → S. For perfectly mixed feed, no dependence on the reaction rates is given (only on the ratio of the reaction rates, which was taken here as constant). The dimensionless Damköhler number for nth-order reactions $\varphi_i = k_i C_{B_0}^{n-1} W^2 / D$ represents the ratio between the reaction rate and the diffusion rate, where $k_i\psi$ is the reaction rate of the step i, C_{B_0} the concentration of reactant B at time zero, W the lamination width and D the diffusion constant. The reaction is the controlling step when $\phi_i < 1$, whereas diffusion is the controlling step when $\phi_i > 10^4$. Thus, for low reaction rates, reaction control is given for a lamination width of 100 µm, sufficient to achieve complete mixing in a time before notable reaction onset. For higher rate constants, diffusion control is given and a decrease in yield with increase in the lamination width and/or the rate constants is observed. The physical state of the reactants can also notably impact such scenario, since the diffusion coefficient in gases is $\sim 10^{-5}$ m^2 s^{-1} and in liquids 10^{-9} m^2 s^{-1}.

The spatial concentration profiles may further be exploited for separation, e.g. by enriching the product in the central channel part and having around that the species to be separated. Hence this permits separation by withdrawal of parts of the laminar flow

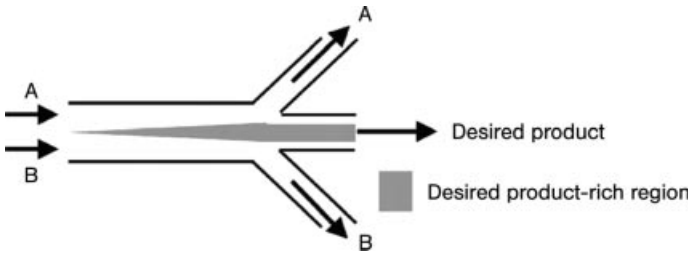

Figure 14.6 Separation of a stream with enrichment of product in the channel middle by withdrawal of parts of the laminar flow via a three-exit fork flow structure. Reprinted with permission from Elsevier [22].

via a fork flow structure (Figure 14.6) – a simple principle which, however, is expected to pose considerable technical expenditure in practice on controlling the flows.

More complex fluid arrangements were analyzed in a further study [23]. As a further dimensionless number, the ratio of channel width to depth, *w*, was introduced, namely the aspect ratio (Figure 14.7). Product yields in reactors with a

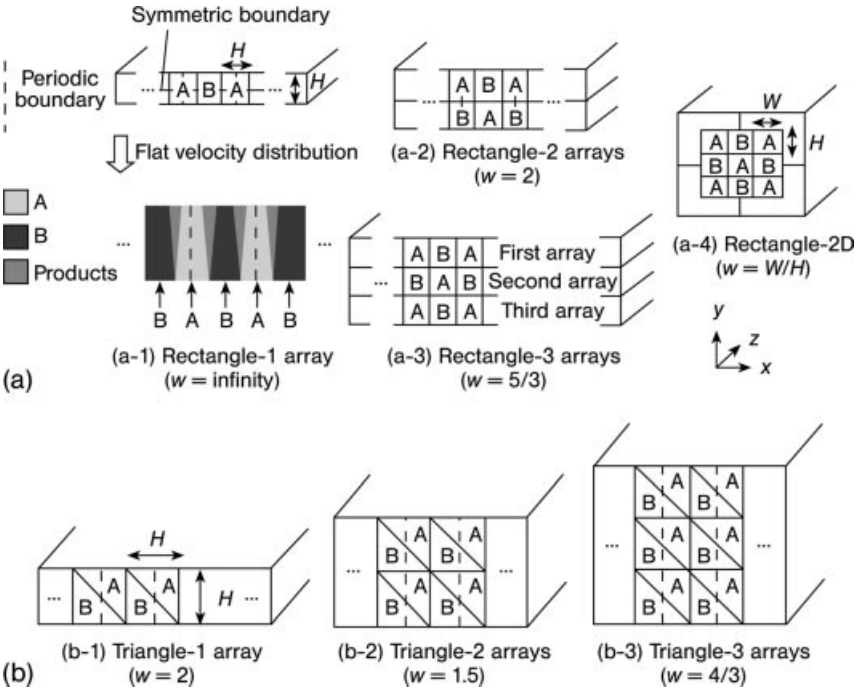

Figure 14.7 Arrangement of fluid segments: (a) rectangle (square); (b) triangle (isosceles right-angled triangle). Reprinted with permission from Wiley-VCH Verlag GmbH [23].

right-angled triangular fluid cross-section have a larger dependence on w than rectangular structured reactors. In addition, it was shown that reactor performance with a laminar velocity distribution is comparable to or exceeds that with a flat velocity distribution, for identical dimensionless numbers. Achieving specifically structured flows with specific channel dimensions is a matter of fabrication efforts and costs in addition to operation issues such as pressure drop and clogging sensitivity. Hence the parametric study performed allows one to choose optimized processing under economic considerations.

The effect of fluid structuring on liquid–solid reactions using a porous catalyst layer was also analyzed, but is not discussed further here, since heterogeneous reactions are outwith the scope of this chapter [20]. See also [24] for a review of the studies discussed above.

14.3.4
Impact of Heat Exchange

Exothermic reactions generate heat which has to be removed. If the heat management is not ideal, the reaction solution is warmed up (hot spots), which promotes side formation by reactions with higher activation energies and thermal follow-up reactions, e.g. decomposition.

Ionic liquid synthesis is performed without a solvent, i.e. just using the pure reactants so that the heat generation is maximum. The alkylation to the ionic liquid ethylmethylimidazole ethylsulfate is such a highly exothermic reaction [25]. A calorimetric-based investigation confirmed fast kinetics. Heat management is a crucial point during the reactor operation to avoid thermal runaway, since even in minichannels huge hot spots of much more than 50 °C emerge. The avoidance of thermal overshooting correlates directly with the quality and purity of the ionic liquid product, as indicated by, e.g., a color change in the case of thermal overshooting. For this reason, dropwise addition of reactant is done in the conventional synthesis in semi-batch stirred-tank reactors, which prolongs the reaction time much above what is kinetically demanded.

For the solvent-free alkylation reaction to ethylmethylimidazole ethylsulfate, a combination of a microstructured reactor system and two tubular capillary reactors has been proposed [25]. This allows a multi-stage reactor design with either different internal diameters or different process parameters, here different cooling temperatures (or a combination of both). In a reaction optimization study, it was found that the best performance was reached using the two tubular capillary reactors at two different cooling temperatures. Safe and stable operation of this reactor system was proven experimentally and rendered ionic liquids of high quality. The specific reactor performance was about 4 kg m^{-3} s^{-1}, being about three orders of magnitude higher than with more traditional reactors. This methodology of reactor optimization is described in a more quantitative way in [26], in particular how to estimate the channel diameter for given kinetics and thermodynamics to avoid run-away.

14.3.5
Impact of Electromagnetic Waves and Alternative Energies

The use of alternative energy forms and transfer mechanisms to microprocessing can intensify a process and allows different functions and applications than does transfer to conventional macroscale processing [27]. There is little doubt that alternative energy sources and forms of energy can intensify a process carried out in microreactors. The main aim, however, is not to miniaturize these devices further, but to accelerate chemical processes to "fit" in microreactors. This can be achieved by reaching higher product yields by combining alternative means of energy provision (e.g. fast heating and fast quenching), by manufacturing new products that are difficult to prepare by conventional methods or simply by reducing or preventing some basic problems of microreactor operation such as fouling. Correspondingly, microreactors with their highly structured, well-defined geometries have the potential to become the primary tool for exploring the field of alternative energy sources and forms for discovering the underlying mechanisms.

Table 14.1 lists the main impact of alternative sources and forms on microprocessing and conventional equipment, mainly given with the example of heterogeneous systems. The use of alternative energy sources is not restricted to microreactors and may impact different figures of merit depending on the type of reactor. Whereas, for instance, high gravity fields mainly lead to improved heat transfer for conventional equipment, their impact is to increase the processing capacity when using microreactors. Other comparisons are also listed.

14.4
Process Design

14.4.1
Combined Reaction–Separation

So far, only a few microdevice-based separation operations have been reported [28–34]. Even less well known is the combination of separation with reaction. In one case, extraction (not reaction) was performed by the use of micromixers, followed by a classical phase separation in laboratory-made minisettlers [35].

One of the first examples of combined reaction–separation processes at the microscale included three reaction steps and two separation steps (Figure 14.8) [35].

The continuous-flow, multi-step microchemical synthesis of carbamates was realized on a chip. A carboxylic acid chloride was converted to the azide in a liquid–liquid segmented-flow configuration. Product purification was performed by a liquid–liquid separator. The azide was converted to an isocyanate by means of the Curtius rearrangement. Toluene as a high-boiling solvent was used to achieve a high operating temperature in order to have sufficient reaction rates in this rate-limiting reaction step. A gas–liquid separation step, solvent stripping, was applied for removal of the high-boiling solvent. The conversion for the Curtius rearrangement was 99% at

Table 14.1 Comparison of the impact of alternative sources and forms on conventional equipment and microreactors. Reprinted with permission from the American Chemical Society [27].

Energy source	Form of application	Intensified element
High-gravity field	Spinning disc reactor	Heat transfer from liquid film
		Mass transfer in liquid film
		Reaction time
		Equipment size
		Impurities level
	Rotating packed bed	Liquid-side mass transfer
		Gas-side mass transfer
Electric field – static	Extraction systems	Heat transfer from droplets
		Mass transfer
		Interfacial area (by emulsification)
	Boiling liquids, evaporators	Heat transfer
Electric field – dynamic (gliding arc)	Gaseous non-catalytic reactions	Energy consumption
		Equipment size
Electromagnetic radiation – microwaves	Liquid-phase (catalytic) reactions	Reaction time
		Product yield
	Gas-phase catalytic reactions	Conversion, product yield
	Distillation	Distillation time
Electromagnetic radiation – light	Photocatalytic reactions	Product yield/selectivity
	Energy (in sunlight-driven processes)	
Acoustic field	Ultrasound irradiation	Reaction time
		Product yield
		Gas–liquid mass transfer
		Liquid–solid mass transfer
	Low-frequency acoustics	Gas–solid mass transfer
		Gas–liquid mass transfer
Flow	Hydrodynamic cavitation	Reaction time and product yield
	Supersonic flow	Gas–liquid mass transfer coefficient
		Fluid-bed reactor capacity

105 °C; however, a 60 min residence time was required, which points to the need to find further high-boiling solvents to achieve still higher temperatures. The carbamate was prepared from the reaction of an alcohol and the isocyanate in a yield of >96%.

14.4.2 Multi-step Reactions

The multi-step synthesis of the alkaloid natural product (±)-oxomaritidine was performed with microfluidic pumping systems feeding various packed columns containing immobilized reagents, catalysts, scavengers or catch-and-release

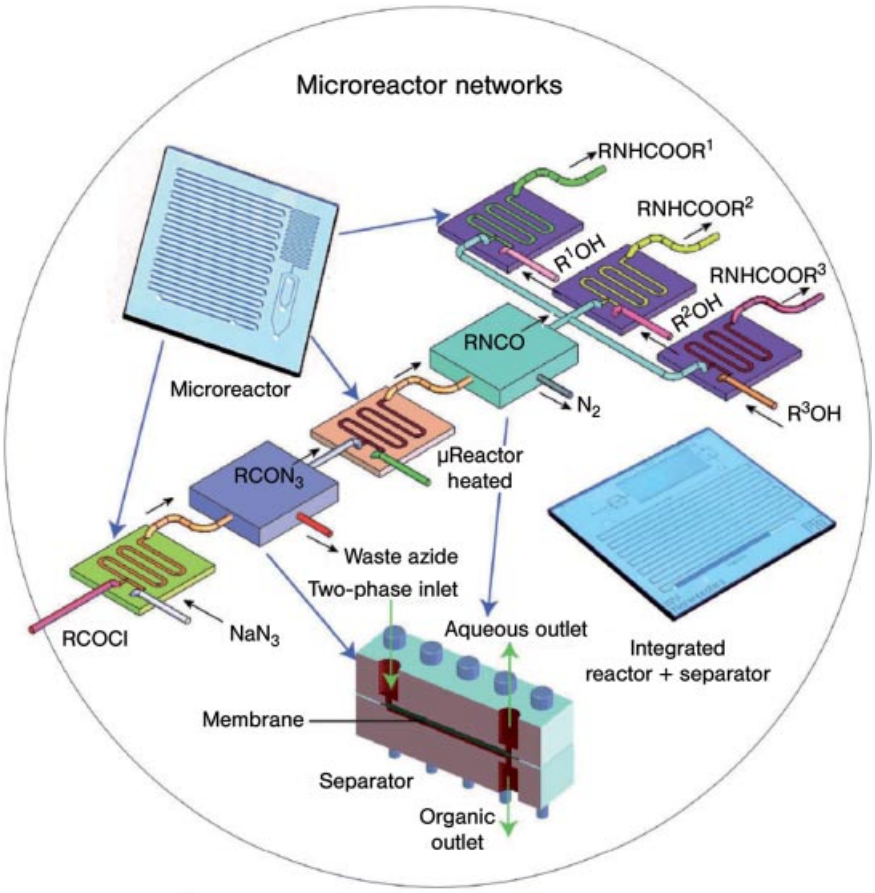

Figure 14.8 Schematic of combined reaction–separation processes on a chip including three reaction steps and two separation steps. Reprinted with permission from Wiley-VCH Verlag GmbH [36].

agents [36]. In this way, seven separate synthetic steps were linked into one continuous process chemistry (Figure 14.9). This involved nucleophilic substitution, oxidation, hydrogenation, trifluoroacylation, ring closure by oxidative phenolic coupling and 1,4-conjugate addition. (±)-Oxomaritidine is a cytotoxic alkaloid of the Amaryllidaceae family of natural products

A yield of 20 mg of reaction product was obtained at 90% purity, as confirmed by ^{1}H NMR spectroscopy. The only impurity was the *ortho*-coupled product derived from the phenolic oxidation, which could be easily separated using preparative HPLC. The yield over the entire sequence was >40%.

Moreover, a flow process for the multi-step assembly of peptides was used to construct a series of Boc, Cbz and Fmoc *N*-protected dipeptides at high yields and purities [38]. This method was extended to the synthesis of a tripeptide derivative.

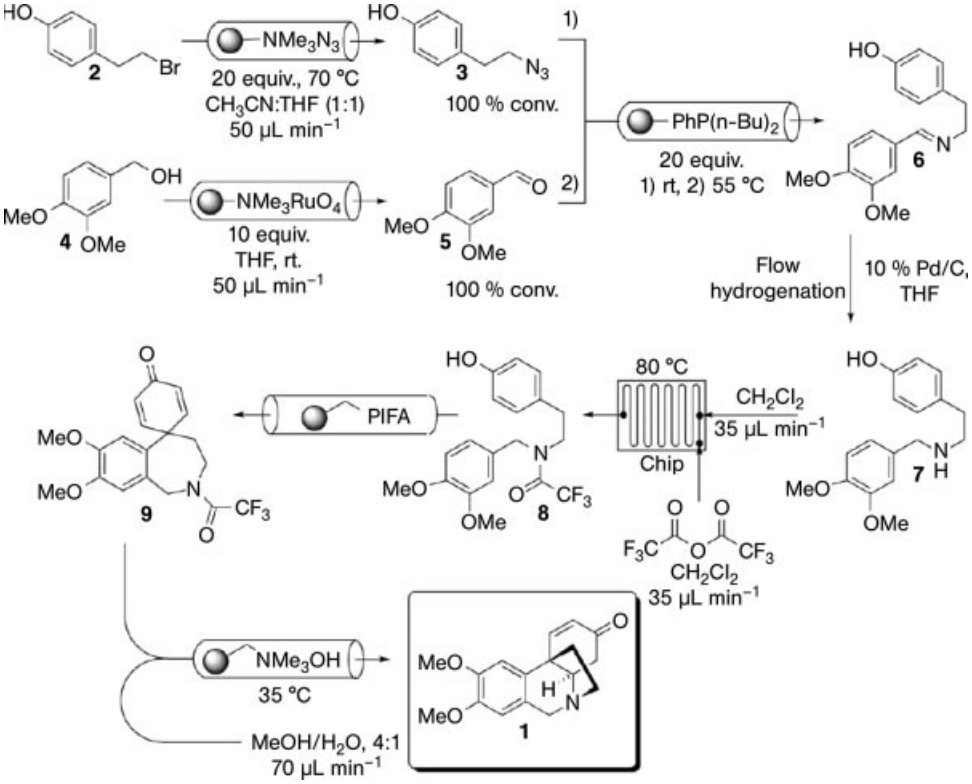

Figure 14.9 Multi-step synthesis of the alkaloid natural product (±)-oxomaritidine by seven steps. Reprinted with permission from the Royal Society of Chemistry [37].

The first enantioselective total synthesis of the 2-aryl-2,3-dihydro-3-benzofurancarboxyamide neolignan grossamide was also developed using a fully automated and scalable flow reactor [39].

14.5 Novel Process Windows

Chemical reactions and processes were performed for centuries with view to using batch technology. The latter is an intrinsically slow technique since a large volume needs to be processed, which simply means that nearly all operations such as stirring and heating need time before reaching their final state. Moreover, for safety reasons when handling large volumes, such operation is further deliberately slowed. The operations often follow each other, which further increases the processing time. In turn, continuous technology performs all steps at the same time. Using miniaturized dimensions permits, in addition, faster mixing, heating or performance of other

functions. Thus, microprocess technology is suited for fast reactions and processes. A short-cut analysis shows that only some of the existing processes are compatible with such a profile; about 20% were stated in [40]. This leads to the conclusion that there is a need to tailor chemical processes "to 'fit' better in microreactors" [27]. The means to do so are, e.g. working under higher temperatures by changing the solvent or more generally by combining high temperatures with high pressures so that liquid-phase operation (without boiling) is accessible (much) above the solvent's boiling point. Other measures are listed in [41]. Some selected paths are exemplified in the following. Most of the new processing paths have in common that these open process windows far away from regular processing. Hence this has been termed "novel process windows".

14.5.1 High Temperatures – Rate Acceleration

The aqueous Kolbe–Schmitt synthesis with resorcinol needs about 2 h to achieve a 50% yield of the product under typical batch conditions with reflux of the solvent water (100 °C) [42]. In a setup with a minitube reactor and microcooler for quenching the reaction, high-temperature conditions at high pressures can be easily realized. Operation up to 200 °C at pressures of 40–70 bar allows a reduction of the reaction time to about 1 min or below with maximum yields of 45%. Similar findings were made for the phloroglucinol-based Kolbe–Schmitt synthesis [43]. Here, decarboxylation is more pronounced at lower temperature, which decreases the yield so that the operating temperature window is smaller, which also shows the limits of the applicability of the novel process window.

A Pd-catalyzed aminocarbonylation was performed above the boiling point of the solvent toluene up to 150 °C [44]. Two reaction products can be generated, an amide and an α-ketoamide, depending on the insertion of one or two equivalents of carbon monoxide. It was demonstrated that high-temperature microreactor operation favors the amide formation and high pressures lead to the α-ketoamide, according to prior literature experience with conventional technology.

Microreactors allow one easily to perform processes at elevated temperatures above the limit of most multipurpose conventional reactors, which is typically ~140 °C [45]. Operation above this limit is only possible by means of special reactors equipped with heat transfer units.

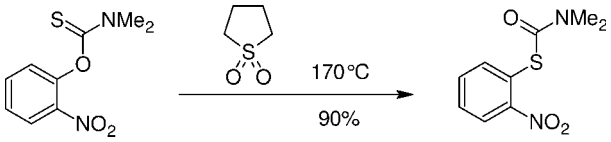

For the Newman–Kuart rearrangement, the reaction temperature could be extended up to 200 °C using microprocess technology. *O*-(2-Nitrophenyl)-*N*,*N*-dimethylthiocarbamate was converted to *S*-(2-nitrophenyl)-*N*,*N*-dimethylcarba-

mothioate at 170 °C in 14 min in 90% yield. Quantitative conversion with a throughput of 34 g h^{-1} was achieved with sulfolane as solvent at the same temperature and reaction time.

14.5.2
High Pressures – Transition State Volume Effects

Volume effects of the transition state, among other mechanistic reasons, drive product selectivity if pressure is applied. This use of high-pressure microprocess technology on its own was demonstrated for a nucleophilic aromatic substitution with a base reacting with a nitrobenzene derivative with various halogens as leaving groups [46]. For pyrrolidine, piperidine and morpholine, strong effects on the reaction rates were found in a pressure operational window up to 600 bar.

Similar effects were found for the stereoselectivity of the Diels–Alder reaction between furylmethanols with maleimides, with pressure changing slightly the *endo*/*exo* ratio of the cycloadducts [46].

The esterification reaction of phthalic anhydride with methanol was performed at different temperatures at pressures up to 110 bar using supercritical CO_2 as co-solvent [47]. By virtue of high pressure, a 53-fold rate enhancement was achieved at 110 bar and 60 °C (i.e. under non-supercritical conditions) as compared with batch experiments at 1 bar at the same temperature. Using in addition supercritical CO_2 gives a 5400-fold increase.

14.5.3
Solventless and Solvent-free Operation

"Solventless" means using highly concentrated solutions, i.e. with the presence of a solvent. This is an established term in some literature and was not created by us here. "Solvent-free" refers to processing without any solvent, but using only the (liquid or liquefied) reactants.

Ionic liquid synthesis is usually performed solvent-free by means of the Menschutkin reaction, i.e. the two reactants (typically a base and an alkyl derivative with leaving group) are mixed and react in the liquid state and yield the liquid product, with almost complete conversion. The challenge for some of these reactions, such as the conversion of methylimidazole and diethyl sulfate (adiabatic temperature rise: 173 K) is the high exothermicity under the high reaction rate [25]. This leads to considerable hot-spot formation with sudden temperature jumps of 100 °C and more. This adversely affects the product quality, as is easily visible by a coloring to yellowish or even brown, and places restrictions on safe process optimization. For these reasons, the reactions may be carried out more slowly than kinetically possible to allow for sufficient heat transfer.

For solvent-free ionic liquid synthesis from methylimidazole and diethyl sulfate, a reactor configuration with an integrated microreactor and two capillaries was developed [25]. This three-fold division of the reaction path serves to compromise

thermal management capability and throughput. The findings of the corresponding kinetic study are described above.

14.5.4
Exploration into Explosive and Thermal Runaway Regimes

The reaction of methyl chloroformate with amines to give methyl carbamates is exothermic and, due to large heat release, hot spots occur [45]. This is even observed at the laboratory scale when using *N*-methoxycarbonyl-L-*tert*-leucine.

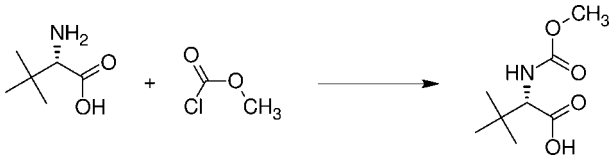

Calorimetric measurements show that the heat release rate is mainly feed controlled, as the square shape of the heat flow curve demonstrates (Figure 14.10) [44]. Whenever feed was added, the heat flow responds without delay.

In case of complete malfunction of cooling and stirring systems, the temperature may exceed the solvent reflux temperature [45]. Accordingly, a slow dosing of the methyl chloroformate is necessary to have control over the heat release. After having determined the reaction parameters at the 1 g scale, the reaction was carried out in a microreactor with 91% yield at a 7 min residence time. More than 1 kg of *N*-methoxycarbonyl-L-*tert*-leucine was prepared within 12 h.

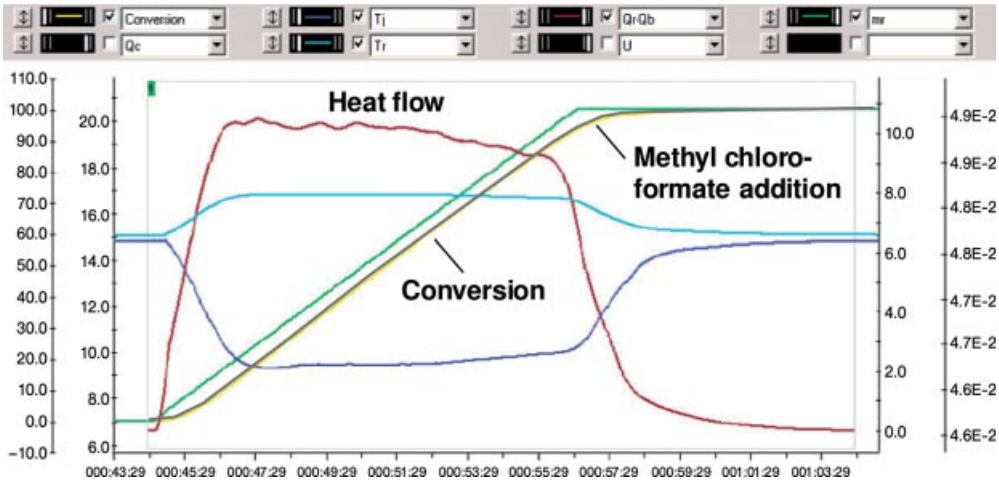

Figure 14.10 Reaction calorimetry results from the addition of methyl chloroformate (slight excess) to L-*tert*-leucine. Reprinted with permission from the American Chemical Society [45].

Microprocess technology has a similar enabling function for the reaction of *N*-Boc-4-piperidone with ethyl diazoacetate, which involves processing hazardous substances [45].

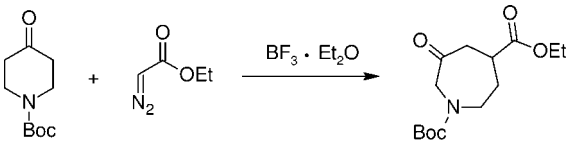

When performed in a batch mode on the 70 mg scale, no safety issues arose and an 81% yield was obtained [45]. Reaction calorimetry revealed a very exothermic reaction after feeding and subsequent mixing with an initiation period, i.e. the response of the heat flow curve was delayed by about 1 min compared with the feed curve. Therefore, the heat release rate with this mode of addition is not feed controlled. The reaction is very sluggish, since the reaction occurs at a single blow as soon as 60% of the material has been added. Calculating the worst-case temperature rise shows that the reaction would rapidly increase in temperature and can approach the solvent reflux temperature, possibly throwing out the reaction mixture in case of cooling or stirring malfunction. This would particularly include the full accidental release of all the $BF_3{\cdot}Et_2O$.

Several heterogeneous reactions, especially performed in the gas phase with risk of explosion or thermal runaway were also safely performed by micro process technology. But this is not discussed here, since the chapter deals only with homogeneous reactions.

14.6
From Laboratory to Production Scale – Scale-out

14.6.1
Numbering-up

Different ways exist for transferring laboratory microprocess operation to the production scale. The most often quoted approach is numbering-up, i.e. the parallel operation of identical microfluidic units to increase throughput. Hydrodynamics and mass and heat transfer are kept the same throughout the whole development cycle and there is no need for time-consuming re-engineering considerations at each stage. Numbering-up can be done by repetition on a device level (e.g. operating several micromixers in parallel) or on a microstructured unit level (e.g. operating several microchannels or more complex shaped microstructures in parallel) [48]. The former approach was termed external numbering-up or even simply numbering-up; the latter means was termed internal numbering-up or equaling-up.

14.6.2
Internal Numbering-up or Equaling-up

Internal numbering-up allows a higher degree of integration to be reached and leads also to a higher degree of parallelization, i.e. gives compact units of high

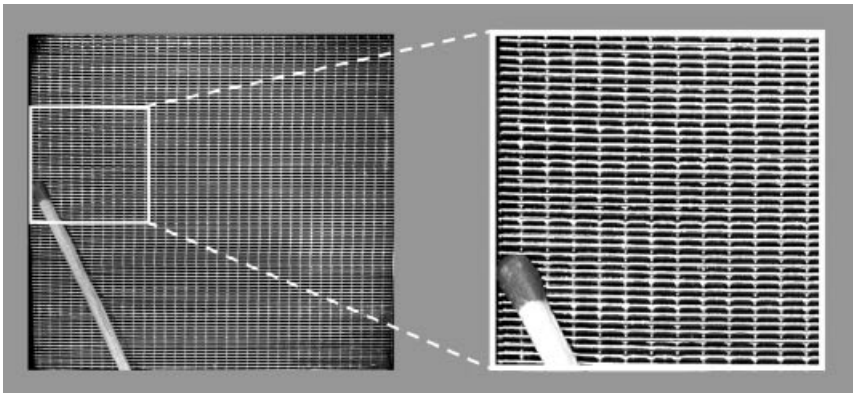

Figure 14.11 Internal numbering-up by parallel assembly of microchannels within a 10 kW microstructured counter-flow heat exchanger; cut view given. Courtesy of IMM.

productivity [47]. This is state of the art for microstructured gas-phase reactors such as reformers or their gas purification counterparts. An autothermal isooctane 5 kW reformer, for example, comprises 25 000 microchannels in a shoebox format [49, 50]. A similar internal structure has a 10 kW microstructured counter-flow heat exchanger (Figure 14.11).

Special measures have to be taken to achieve a uniform gas distribution such as shaping the diffusers or even using more complex flow manifold structures, e.g. a thick-walled screen header (Figure 14.12) [51–54].

For the case of the homogeneous reactions considered in this chapter (the majority being in the liquid phase), parallel channel arrangements were also developed. Most often, a low degree of parallelization is needed to achieve the desired throughput, e.g. less than 10. This is used, for example, in several split-and-recombine mixers such as the fork-mixer array [55].

Other mixer concepts use a much higher degree of parallelization by stacking several hundred plates with identical or periodically changed microstructured units. Examples are the V-type microstructured mixers with alternately tilted channels [56], cross-flow micro heat exchangers [9] and the so-called StarLaminator microstructured mixers [57], creating multiple microjets which enter a larger main stream. In the last two cases, throughputs as high as several thousand liters per hour were reported. For one StarLaminator mixer, a capacity of even 30 000 $L\,h^{-1}$ was targeted.

Equaling-up has been applied to connect several capillaries of sub-millimeter or millimeter internal dimensions, e.g. in a stage-wise fashion. This concept was applied especially by Japanese researchers for their pilot plants, e.g. for radical polymerization [58]. As an alternative concept, the same researchers proposed multi-tube arrangements, tightly packed in a housing, similar to the macroscopic tube-and-shell heat exchangers. Such multi-tube blocks can be arranged in a sequential manner, with varying tube diameters (and length), to give a multi-scale design.

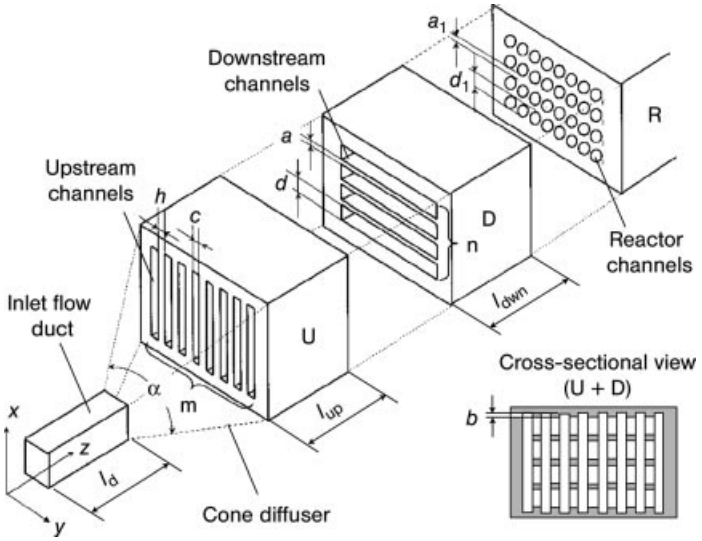

Figure 14.12 Scale-out of gas flows by internal numbering-up via a flow manifold module: Cone diffuser (I), thick-walled screen (II), eight reactor compartments (III), insulating ring (IV), outlet flow confuser (V) and sampling section (VI). Reprinted with permission from Wiley-VCH Verlag GmbH [52].

14.6.3
External Numbering-up: Device Parallelization

Although the equaling-up concept is appealing at first sight, there are good reasons for relying on external numbering-up of devices [48]. Equaled-up devices, if they do not exist at the time of demand, have to be developed, which involves time, costs and development risks. Especially for small capacity increases, connecting well-characterized existing devices is a more practical approach. Flow distribution can be done using physically separate, well-characterized manifolds as opposed to the more complex task of integrated microstructured flow distribution structures.

For the Merck production case with the enolate synthesis performed as a micro-process step, five parallel minimixers were sufficient [59]. For a polyacrylate pilot plant, 28 interdigital micromixers were connected, grouped into four groups each with eight micromixers [60].

14.6.4
Smart Scale-up

Although some reviewers tend to describe the numbering-up approach as inherent to microprocess technology, continuous processing at a small scale can also be done with families of devices with a slight increase in characteristic inner diameter. The scale-up factor is often not larger than five. Still, through the volume flow-to-pressure loss dependence, this results in a large gain in throughput.

Examples are the class of caterpillar micromixers, exploiting recirculation patterns, with the channel width and depth (the ramp width and depth, respectively) being increased for each member [2, 4]. Also for the StarLaminator series, throughput can be increased by increasing the platelet width and thickness (in addition to having more platelets) [57]. The Merck production case quoted above is an example of a smart increase in dimensions [58]. For laboratory investigations, interdigital micromixers with feed channels of 25 μm width and a mixing channel of 500 μm diameter were used, whereas for production minimixers with internals probably in the millimeter range were used (the exact dimensions were not given).

14.6.5 Multi-scale Architecture

Typically, most of the heat produced during a reaction is released at the beginning and then the heat production gradually decreases. Other scenarios are also possible, e.g. with a certain activation delay at the beginning and then accompanied by a sudden, even stronger release of heat. Anyhow, since the heat production varies with time, continuous-flow processing offers the possibility to segment the flow path to achieve a stage-wise response by reactor design. This implies not only varying a characteristic dimension by choosing members within one family of microreactors. For practical reasons (e.g. availability), connections between different types of microreactors (e.g. from integrated reactors to capillaries) or even from microreactors to conventional reactors (e.g. static mixers) are made. This mix of different reactors with different scales to achieve best-practice chemical processing is commonly referred to as multi-scale reactor architecture [25].

Multi-scale processing may be done for reasons other than to control exothermic reactions, e.g. for staged post-mixing, to have different process parameter levels along the reaction path (stage-wise change of temperature, pressure, etc.) or to combine various unit operations with different demands on process intensification [25].

References

1 W. Ehrfeld, V. Hessel, H. Löwe, *Microreactors*, Wiley-VCH Verlag GmbH, Weinheim, **2000**.

2 V. Hessel, S. Hardt, H. Löwe, *Chemical Micro Process Engineering - Fundamentals, Modelling and Reactions*, Wiley-VCH Verlag GmbH, Weinheim, **2004**.

3 V. Hessel, C. Serra, H. Löwe, G. Hadziioannou, Polymerizationen in mikrostrukturierten Reaktoren: Ein Überblick. *Chem. Ing. Tech.*, **2005**, *77* (11), 1693–1714.

4 V. Hessel, H. Löwe, A. Müller, G. Kolb, *Chemical Micro Process Engineering – Processing, Applications and Plants*, Wiley-VCH Verlag GmbH, Weinheim, **2005**.

5 G. Kolb, *Fuel Processing*, Wiley-VCH Verlag GmbH, Weinheim, **2008**.

6 S.-R. Deibel, Schneller planen, rascher produzieren – Paradigmenwechsel in der Anlagen-Philosophie erwartet. *CHEManager*, **2006**, *2*.

7 A. M. Thayer, Harnessing microreactions. *Chem. Eng. News*, **2005**, *83* (22), 43–52.

8 V. Hessel, H. Löwe, F. Schönfeld, Micromixers – a review on passive and active mixing principles. *Chem. Eng. Sci.*, **2006**, *60*, 2479–2501.

9 K. Schubert, J. Brandner, M. Fichtner, G. Linder, U. Schygulla, A. Wenka, Microstructure devices for applications in thermal and chemical process engineering. *Microscale Thermophys. Eng.*, **2001**, *5*, 17–39.

10 P. Löb, V. Hessel, U. Krtschil, H. Löwe, Continuous micro-reactor rigs with capillary sections in organic synthesis. *Chim. Oggi – Chem. Today*, **2006**, *24* (2), 46–50.

11 P. Guichardon, L. Falk, Characterization of micromixing efficiency by the iodide-iodate reaction system. Part I: experimental procedure. *Chem. Eng. Sci.*, **2000**, *55*, 4233–4243.

12 A. Renken, Mikrostrukturierte Reaktoren, in *Technische Chemie*, ed. M. Baerns, A. Behr, A. Brehm, J. Gmehling, H. Hofmann, U. Onken and A. Renken, Wiley-VCH Verlag GmbH, Weinheim, Chapter 6.3, **2006**, pp. 218–226

13 F. Trachsel, A. Günther, S. Khan, K. F. Jensen, Measurement of residence time distribution in microfluidic systems. *Chem. Eng. Sci.*, **2005**, *60*, 5729–5737.

14 K. Golbig, A. Kursawe, M. Hohmann, S. Taghavi-Moghadam, T. Schwalbe, Designing microreactors in chemical synthesis – residence-time distribution of microchannel devices. *Chem. Eng. Commun.*, **2005**, *192*, 620–629.

15 M. Günther, S. Schneider, J. Wagner, R. Gorges, Th. Henkel, M. Kielpinski, J. Albert, R. Bierbaum, J. M. Köhler, Characterization of residence time and residence time distribution in chip reactors with modular arrangements by integrated optical detection. *Chem. Eng. J.*, **2004**, *101*, 373–378.

16 C. Amador, D. Wenn, J. Shaw, A. Gavriilidis, P. Angeli, Design of a mesh microreactor for even flow distribution and narrow residence time distribution. *Chem. Eng. J.*, **2007**, *135*, 259–269.

17 S. Lohse, I. Gerlach, D. Janasek, P. S. Dittrich, D. W. Agar, *presented at IMRET, 9 Potsdam*, **2006**.

18 S. Lohse, B. T. Kohnen, D. Janasek, P. S. Dittrich, J. Franzke, D. W. Agar, A novel method for determining residence time distribution in intricately structured microreactors. *Lab Chip*, **2008**, *8*, 431–438.

19 P. H. Paul, M. G. Garguilo, D. J. Rakestraw, Imaging of pressure- and electrokinetically driven flows through open capillaries. *Anal. Chem.*, **1998**, *70*, 2459–2467.

20 A. Rouge, B. Spoetzl, K. Gebauer, R. Schenk, A. Renken, Microchannel reactors for fast periodic operation: the catalytic dehydration of isopropanol. *Chem. Eng. Sci.*, **2001**, *56*, 1419–1427.

21 J.-M. Commenge, T. Obein, G. Genin, X. Framboisier, S. Rode, V. Schanen, P. Pitiot, M. Matlosz, Gas-phase residence time distribution in a falling-film microreactor. *Chem. Eng. Sci.*, **2006**, *61*, 597–604.

22 N. Aoki, S. Hasebe, K. Mae, Mixing in microreactors: effectiveness of lamination segments as a form of feed on product distribution for multiple reactions. *Chem. Eng. J.*, **2004**, *101*, 323–331.

23 N. Aoki, S. Hasebe, K. Mae, Geometric design of fluid segments in microreactors using dimensionless numbers. *AIChE J.*, **2006**, *52*, 1502–1515.

24 K. Mae, Advanced chemical processing using microspace. *Chem. Eng. Sci.*, **2007**, *62*, 4842–4851.

25 A. Renken, V. Hessel, P. Löb, R. Miszczuk, M. Uerdingen, L. Kiwi-Minsker, Ionic liquid synthesis in a microstructured reactor for process intensification. *Chem. Eng. Process.*, **2007**, *46*, 840–845.

26 A. Renken, L. Kiwi-Minsker, Chemical reactions in continuous flow micro-structured reactors, in *Micro Process Engineering* ed. N. Kockmann, Wiley-VCH Verlag GmbH, Weinheim, **2006**, pp. 173–201.

27 A. Stankiewicz, Energy matters: alternative sources and forms of energy for intensification of chemical and biochemical processes. *Trans. IChemE,*

Chem. Eng. Res. Des., **2006**, *84* (A7), 511–521.

28 J. G. Kralj, R. Hemantkumar, R. Sahoo, K. F. Jensen, Integrated continuous microfluidic liquid–liquid extraction. *Lab Chip*, **2007**, *7*, 256–263.

29 S. K. Cho, Y. Zhao, C.-J. Kim, Concentration and binary separation of micro particles for droplet-based digital microfluidics. *Lab Chip*, **2007**, *7*, 490–498.

30 B. A. Wilhite, S. E. Weiss, J. Y. Ying, M. A. Schmidt, K. F. Jensen, High-purity hydrogen generation in a microfabricated 23 wt% Ag–Pd membrane device integrated with 8:1 $LaNi_{0.95}Co_{0.05}O_3$/Al_2O_3 catalyst. *Adv. Mater.*, **2006**, *18*, 1701–1704.

31 M. Zimmermann, S. Bentley, H. Schmidt, P. Hunziker, E. Delamarche, Continuous flow in open microfluidics using controlled evaporation. *Lab Chip*, **2005**, *5*, 1355–1359.

32 J. D. Ramsey, G. E. Collins, Integrated microfluidic device for solid-phase extraction coupled to micellar electrokinetic chromatography system. *Anal. Chem.*, **2005**, *77*, 6664–6670.

33 A. Aota, M. Nonaka, A. Hibara, T. Kitamori, Countercurrent laminar microflow for highly efficient solvent extraction. *Angew. Chem. Int. Ed.*, **2007**, *46*, 878–880.

34 T. Manabu, T. Minagawa, T. Kitamori, Integration of a microextraction system. Solvent extraction of a Co–2-nitroso-5-dimethylaminophenol complex on a microchip. *J. Chromatogr. A*, **2000**, *894*, 19–23.

35 K. Benz, K.-J. Regenauer, K.-P. Jäckel, J. Schiewe, W. Ehrfeld, H. Löwe, V. Hessel, Utilization of micromixers for extraction processes. *Chem. Eng. Technol.*, **2001**, *24*, 11–17.

36 H. R. Sahoo, J. G. Kralj, K. F. Jensen, Multistep continuous flow microchemical synthesis involving multiple reactions and separations. *Angew. Chem. Int. Ed.*, **2007**, *46*, 5704–5708.

37 I. R. Baxendale, J. Deeley, C. M. Griffiths-Jones, S. V. Ley, S. Saaby, G. K. Tranmer, A flow process for the multi-step synthesis of the alkaloid natural product oxomaritidine: a new paradigm for molecular assembly. *Chem. Commun.*, **2006**, 2566–2568.

38 I. R. Baxendale, S. V. Ley, C. D. Smith, G. K. Tranmer, A flow reactor process for the synthesis of peptides utilizing immobilized reagents, scavengers and catch and release protocols. *Chem Commun.*, **2006**, 4835–4837.

39 I. R. Baxendale, C. M. Griffiths-Jones, S. V. Ley, G. K. Tranmer, Preparation of the neolignan natural product grossamide by a continuous-flow process. *SynLett.*, **2006**, *3*, 427–430.

40 D. M. Roberge, L. Ducry, N. Bieler, P. Cretton, B. Zimmermann, Microreactor technology: a revolution for the fine chemical and pharmaceutical industries? *Chem. Eng. Technol.*, **2005**, *28*, 318–323.

41 V. Hessel, P. Löb, H. Löwe, Development of microstructured reactors to enable organic synthesis rather than subduing chemistry. *Curr. Org. Chem.*, **2005**, *9*, 765–787.

42 V. Hessel, C. Hofmann, P. Löb, J. Löhndorf, H. Löwe, A. Ziogas, Aqueous Kolbe–Schmitt synthesis using resorcinol in a micro-reactor laboratory rig under high-*p*,*T* conditions. *Org. Process Res. Dev.*, **2005**, *9*, 479–489.

43 V. Hessel, C. Hofmann, P. Löb, H. Löwe, M. Parals, Microreactor processing for the aqueous Kolbe–Schmitt synthesis of hydroquinone and phloroglucinol. *Chem. Eng. Technol.*, **2007**, *30*, 355–362.

44 E. R. Murphy, J. R. Martinelli, N. Zaborenko, S. L. Buchwald, K. F. Jensen, Accelerating reactions with microreactors at elevated temperatures and pressures: profiling aminocarbonylation reactions. *Angew. Chem. Int. Ed.*, **2007**, *119*, 1764–1767.

45 X. Zhang, S. Stefanick, F. J. Villani, Application of microreactor technology in process development. *Org. Process Res. Dev.*, **2004**, *8*, 455–460.

46 F. Benito-Lopez, High pressure: a challenge for lab-on-a-chip technology, PhD Thesis, University of Twente., **2007**.

47 F. Benito-Lopez, R. M. Tiggelaar, K. Salbut, J. Huskens, R. J. M. Egberink, D. N. Reinhoudt, H. J. G. E. Gardeniers, W. Verboom, Substantial rate enhancements of the esterification reaction of phthalic anhydride with methanol at high pressure and using supercritical CO_2 as a co-solvent in a glass microreactor. *Lab Chip*, **2007**, *10*, 1345–1351.

48 R. Schenk, V. Hessel, C. Hofmann, J. Kiss, H. Löwe, F. Schönfeld, Numbering-up of micro devices: a first liquid-flow splitting unit. *Chem. Eng. Technol.*, **2003**, *26*, 1271–1280.

49 G. Kolb, T. Baier, J. Schürer, D. Tiemann, A. Ziogas, H. Ehwald, P. Alphonse, A micro-structured 5 kW complete fuel processor for iso-octane as hydrogen supply system for mobile auxiliary power units: Part I. Development of autothermal reforming catalyst and reactor. *Chem. Eng. J.*, **2007**, *138*, 474–489.

50 G. Kolb, T. Baier, J. Schürer, D. Tiemann, A. Ziogas, S. Specchia, C. Galletti, G. Germani, Y. Schuurman, A micro-structured 5 kW complete fuel processor for iso-octane as hydrogen supply system for mobile auxiliary power units: Part II. Development of water-gas shift and preferential oxidation catalysts reactors and assembly of the fuel processor. *Chem. Eng. J.*, **2007**, *138*, 653–663.

51 M. J. M. Mies, E. V. Rebrov, M. H. J. M. de Croon, J. C. Schouten, Microreactor for rapid parallel testing of catalysts, *Int. Pat. Appl. WO 2006/107206*, **2006**.

52 E. V. Rebrov, I. Z. Ismagilov, R. P. Ekatpure, M. H. J. M. de Croon, J. C. Schouten, Header design for flow equalization in microstructured reactors. *AIChE J.*, **2007**, *53*, 28–38.

53 E. V. Rebrov, I. Z. Ismagilov, R. P. Ekatpure, M. H. J. M. de Croon, J. C. Schouten, Design of a thick-walled screen for flow equalization in microstructured reactors. *J. Micromech. Microeng.*, **2007**, *17*, 633–641.

54 M. J. M. Mies, E. V. Rebrov, L. Deutz, C. R. Kleijn, M. H. J. M. de Croon, J. C. Schouten, Experimental validation of the performance of a microreactor for the high-throughput screening of catalytic coatings. *Ind. Eng. Chem. Res.*, **2007**, *46*, 3922–3931.

55 S. Panic, S. Loebbecke, T. Tuercke, J. Antes, D. Boskovic, Experimental approaches to a better understanding of mixing performance of microfluidic devices. *Chem. Eng. J.*, **2004**, *101*, 409–419.

56 P. Pfeifer, L. Bohn, O. Görke, K. Haas-Santo, U. Schygulla, K. Schubert, Microstructured mixers for gas-phase processes – manufacture, characterization and application. *Chem. Eng. Technol.*, **2005**, *28*, 439–445.

57 Y. Men, V. Hessel, P. Löb, H. Löwe, B. Werner, T. Baier, Determination of the segregation index to sense the mixing quality of scale-up concepts for pilot- and production-scale microstructured mixers. *Chem. Eng. Res. Des.*, **2006**, *85* (A5), 1–8.

58 T. Iwasaki, N. Kawano, J.-I. Yoshida, Radical polymerization using micro flow system. Numbering-up of microreactors and continuous operation. *Org. Process Res. Dev.*, **2006**, *10*, 1126–1131.

59 H. Krummradt, U. Kopp, J. Stoldt, Experiences with the use of microreactors in organic synthesis, in *Microreaction Technology: 3rd International Conference on Microreaction Technology, Proceedings of IMRET 3*, ed. W. Ehrfeld, Springer, Berlin, **2000**. pp. 181–186.

60 T. Bayer, D. Pysall, O. Wachsen, Micro mixing effects in continuous radical polymerization, in *Microreaction Technology: 3rd International Conference on Microreaction Technology, Proceedings of IMRET 3*, ed. W. Ehrfeld, Springer, Berlin, **2000**, pp. 165–170.

61 R. Aris, On the Dispersion of a Solute in a Fluid Flowing through a Tube. *Proc. Roy. Soc. A.*, **1956**, *235*, 67–77; G. Taylor, Dispersion of soluble matter in solvent flowing slowly through a tube. *Proc. Roy. Soc. A.*, **1953**, *219*, 186–203.